The Bag-1 inhibitor, Thio-2, reverses an atypical 3D morphology driven by Bag-1L overexpression in a MCF-10A model of ductal carcinoma *in situ*

Papadakis E. S.[1]*‡, Barker C. R.[1]*, Syed H.[1], Reeves T.[1], Schwaiger S.[3], Stuppner H.[3], Troppmair J.[4], Blaydes J. P.[1]† and Cutress R. I.[1,2]†‡

[1]Cancer Research UK Centre Cancer Sciences Unit and [2]University Hospital Southampton, University of Southampton Faculty of Medicine, Southampton General Hospital, Southampton, United Kingdom, [3]Institute of Pharmacy/Pharmacognosy, Centre of Molecular Biosciences, University of Innsbruck, Innrain 80-82, A-6020 Innsbruck, Austria, [4]Daniel Swarovski Research Laboratory, Department of Visceral-, Transplant- and Thoracic Surgery, Innsbruck Medical University, Austria

*ESP and CRB contributed equally to this work; † JPB and RIC are joint senior authors

Running Title: A Bag-1L driven 3D breast cell premalignant model

Funding Source: Breast Cancer Campaign project grants (2011NovPR39 and 2010NovPR12)

‡ Corresponding authors: R. I. Cutress (r.i.cutress@soton.ac.uk) and E. S. Papadakis (e.s.papadakis@soton.ac.uk), Cancer Research UK Centre, Cancer Sciences Unit, University of Southampton Faculty of Medicine, Southampton General Hospital, Tremona Road, Southampton SO16 6YD, UK

Telephone: +44 (0)23 8120 6184; Fax: +44 (0)23 8079 5152

Conflict of Interest – The authors declare no conflict of interest

3,474 words (excluding abstract, figure legends acknowledgements and references), 5 figures

Abstract

Mammary MCF-10A cells seeded on reconstituted basement membrane form spherical structures with a hollow central lumen termed acini which are a physiologically-relevant model of mammary morphogenesis. Bcl-2 associated athanogene 1 (Bag-1) is a multifunctional protein overexpressed in breast cancer and ductal carcinoma *in situ* (DCIS). When present in the nucleus Bag-1 is predictive of clinical outcome in breast cancer. Bag-1 exists as three main isoforms, which are produced by alternative translation initiation from a single mRNA. The long isoform of Bag-1, Bag-1L, contains a nuclear localisation sequence not present in the other isoforms. When present in the nucleus Bag-1L, but not the other Bag-1 isoforms, can interact with and modulate the activities of oestrogen, androgen, and vitamin D receptors, Overexpression of Bag-1 mRNA in MCF-10A, is known to produce acini with luminal filling reminiscent of DCIS. As this mRNA predominantly overexpresses the short isoform of Bag-1, Bag-1S, we set out to examine whether the nuclear Bag-1 isoform is sufficient to drive premalignant change by developing a Bag-1L overexpressing MCF-10A model. Two clones differentially overexpressing Bag-1L were grown in 2D and 3D cultures and compared to an established model of HER2-driven transformation. In 2D cultures, Bag-1L overexpression reduced proliferation but did not affect insulin responsiveness or clonogenicity. Acini formed by Bag-1L-overexpressing cells exhibited reduced luminal clearing when compared to controls. An abnormal branching morphology was also observed which correlated with the level of Bag-1L overexpression suggesting further malignant change. Treatment with Thio-2, a small-molecule inhibitor of Bag-1 reduced the level of branching. In summary, 3D cultures of MCF-10A mammary epithelial cells overexpressing Bag-1L demonstrate a premalignant phenotype with features of DCIS. Using this model to test the small molecule Bag-1 inhibitor, Thio-2, reveals its potential to reverse the atypical branched morphology of acini which characterises this premalignant change.

Keywords

Breast cancer, DCIS, Bag-1, HER2, MCF-10A, acini

Abbreviations

Bag-1: Bcl-2 associated anthogene-1, ER: oestrogen receptor, HER2: human epidermal growth factor receptor 2

Introduction

Investigation of breast cancer progression has traditionally relied on two-dimensional (2D) *in vitro* cell models to elucidate the molecular drivers associated with this disease. However, 2D culture has spatial and cell differentiation limitations.[10, 21] 3D cell models provide an important additional experimental tool as they recapitulate several aspects of normal and tumour tissue architecture. When seeded in reconstituted basement membrane (BM), human mammary epithelial normal cells or non-tumourigenic cell lines, such as MCF-10A, follow a highly-regulated morphogenetic program to form organised growth-arrested 3D spherical structures with a central lumen termed acini.[9, 32] This involves polarisation of BM-attached outer cells with concomitant anoikis and metabolic changes of luminal cells that are no longer in contact with the BM (BM-detached).[8, 37] Expression analysis of acini morphogenesis has led to the identification of a 3D molecular signature, comprising genes that are downregulated during this process, which accurately predicts outcome in breast cancer patients.[13, 25]

Contrary to normal breast cells, breast tumour cells and breast cancer cell lines continue to proliferate and give rise to larger acini with altered external morphology and no central lumen due to defects in anoikis and metabolism of BM-detached cells;[21, 27, 32, 37] these structures bear features of ductal carcinoma *in situ* (DCIS), a precursor to invasive ductal carcinoma.[5] Comparison of the transcriptional profiles of a panel of human breast cancer cell lines correlates with their 3D morphology and enables clustering into four main phenotypic subclasses, which are associated with clinically distinct subgroups.[21] The majority of basal B subtype cell lines form invasive stellate structures, which lack E-cadherin and EGFR/HER2 expression, while luminal and basal A subtypes form round, mass, or grape-like structures, which typically overexpress HER2, a marker of poor prognosis in breast cancer.[21, 42] Consistent with this, HER2 overexpression or activation in MCF-10A cells results in atypical, grape-like acinar morphology and impedes lumen formation by attenuating apoptosis and by

driving metabolic changes in BM-detached cells.[16, 27, 33, 36, 37] Culture of MCF10A cells in 3D therefore constitutes a powerful tool for the study of oncogene-driven premalignant changes.

The co-chaperone protein Bcl-2-associated athanogene 1 (Bag-1) is expressed at low levels in most human tissues[43] but is frequently overexpressed in invasive breast carcinoma and importantly also within the preinvasive DCIS stage.[4, 43-45, 47] In the clinical setting of breast cancer, Bag-1 mRNA is a prognostic biomarker included within the Oncotype DX and PAM50 multigene assays[30, 31] and high nuclear Bag-1 immunoreactivity is an independent predictor of outcome and enhances the predictive power of IHC4 score (a combination of the prognostic information from ER, PgR, Ki67 and HER2 immunohistochemical staining).[1, 6, 26, 28, 47] At the cellular level, Bag-1 interacts with a number of protein partners including Bcl-2, Hsc70/Hsp70 chaperones and nuclear hormone receptors to promote cell survival.[46] Proof-of-principle studies from our laboratory have shown that it is possible to restrict breast cancer and melanoma cell growth by targeting Bag-1 protein-protein interactions using synthetic peptides and small-molecule compounds, like Thioflavin S and its biologically active constituent Thio-2.[11, 39, 40] Bag-1 exists as three main isoforms Bag-1S and Bag-1M, which are mainly localised in the cytoplasm, and Bag-1L, which contains a nuclear localisation signal not present in the other isoforms and is predominantly localised in the nucleus.[4, 22, 29, 38, 43, 48] Bag-1L, but not Bag-1M or Bag-1S, enhances the transcriptional activity of androgen receptor,[14, 22, 41] vitamin D receptor[24] and oestrogen receptor.[6] Xenograft studies show that Bag-1L overexpression drives growth of breast tumours formed by oestrogen-responsive ZR-75-1 breast cancer cells in an oestrogen-dependent manner.[23] Although clinical studies and mouse models have shed some light on the role of Bag-1L in breast cancer pathology, little is known about the role of Bag-1L in initiating premalignant change in the breast.

Studies using a 3D cell culture model have shown that concomitant co-overexpression of the main Bag-1 isoforms (Bag-1S, Bag-1M and Bag-1L) in MCF-10A cells leads to the formation of lumenless acini, through attenuation of anoikis in BM-detached cells, but without the

grape like abnormalities in morphology seen with HER2 overexpression. However, there is currently no evidence on the ability of individual Bag-1 isoforms to regulate acinar morphology.[2] Based on published data supporting an important role of nuclear Bag-1L in breast cancer, in this study we sought to examine the effect of the individual Bag-1L isoform on acinar morphogenesis in order to elucidate and describe its role in promoting premalignant change in 3D. We then examined the effect of a small molecule inhibitor of Bag-1, Thio-2, in Bag-1L driven premalignant change in this experimental model of DCIS to determine if these changes might be amenable to therapeutic intervention.

Results

Characterisation of Bag-1L overexpression in 2D culture

To examine the potential role of Bag-1L in breast tumourigenesis, MCF-10A stable cell clones were generated by transfection of a pcDNA3 vector containing Bag-1 cDNA with an optimised Bag-1L start site.[6] Immunoblot analysis revealed the presence of two clones overexpressing Bag-1L at low (Bag-1L/A) and high (Bag-1L/B) levels compared to two pcDNA-containing clones of which clone 1, designated pcDNA, was used as a control for this study (Figure 1a). Immunofluorescence staining revealed higher but heterogeneous expression of Bag-1 in the nucleus of both clones compared to pcDNA and was more intense in Bag-1L/B (Figure 1b), which is consistent with overexpression of Bag-1L.

To characterise the effect of Bag-1L overexpression in 2D culture, cell morphology, colony forming efficiency, and proliferation were examined. Cell clones assumed a cobblestone appearance typically observed in parental MCF-10A cells with lamellipodia extending from the edges of clusters[9] (Figure 1c). Bag-1L overexpression did not alter the colony forming efficiency of MCF-10A cells (Figure 1d) and supported neither anchorage-independent growth *in vitro* nor tumour growth *in vivo* (data not shown). Moreover, Bag-1L/B cells displayed a significant decrease in proliferation compared to pcDNA, as shown by a 38% reduction in crystal violet absorbance, whereas Bag-1L/A cells proliferated comparably to pcDNA controls (Figure 1e).

Effect of Bag-1L overexpression on acini morphogenesis

MCF-10A acini provide a physiologically relevant model to study the influence of Bag-1L overexpression on 3D morphology. Compared to pcDNA acini, Bag-1L protein level was 9-fold higher in Bag-1L/A and 16-fold higher in Bag-1L/B, thereby providing a basis for the study of Bag-1L in acini morphogenesis (Figure 2a). Confocal microscopy images at day 20

of culture indicated formation of a central lumen in MCF-10A parental and pcDNA acini as expected (Figure 2b). In contrast, 26% of Bag-1L/A and 86% of Bag-1L/B acini were lumenless and significantly more abundant than the basal 9% lumenless acini formed by pcDNA cells (Figure 2b, c). Moreover, phase-contrast microscopical examination revealed that 16% of Bag-1L/A and 86% of Bag-1L/B acini assumed a branched morphology (Figure 2d, e), which resembled an atypical phenotype in breast cancer cells reported by Kenny *et al.*.[21] Quantification of confocal and phase-contrast data indicated that the increase in Bag-1L expression observed between Bag-1L/A and Bag-1L/B clones is associated with a significant 3.3-fold increase in the number of atypical acini formed with no central lumen (Figure 2c) and with altered external morphology (Figure 2e).

To further characterise the effect of Bag-1L overexpression on acinar phenotype, cell proliferation and apoptosis were examined by immunofluorescence staining (Figure 3). At day 6 of culture, Ki-67, a protein marker of proliferation,[15] was present in BM-attached cells situated at the periphery of control and Bag-1L/A-overexpressing acini, while in Bag-1L/B-overexpressing acini it was present throughout (Figure 3a). At day 20 of culture, cells in control and Bag-1L-overexpressing acini exhibited minimal Ki67 staining consistent with the induction of growth arrest (Figure 3a). In addition, luminal apoptosis which was detected by M30 (antibody recognising caspase-cleaved cytokeratin 18) was markedly increased in parental and pcDNA acini but was almost undetectable in Bag-1L/A and Bag-1L/B acini (Figure 3b) at day 10 of culture. Taken together, these data show that overexpression of the Bag-1L isoform promotes an atypical acinar phenotype, as it impedes formation of a central lumen, by maintaining proliferation and attenuating apoptosis, and induces a branched acini morphology.

Effect of HER2 overexpression on acini morphogenesis and comparison of 2D growth response to growth factors between Bag-1L- and HER2-overexpressing MCF-10A cells

We next compared the 3D phenotypic changes observed in response to Bag-1L overexpression to a described and recognised[27, 33] 3D model of HER2 transformation that we generated. HER2 protein overexpression was confirmed by immunoblotting (Figure 4a) and immunofluorescence staining (Figure 4b). Lumen formation in acini grown to day 12 and stained with phalloidin was examined by confocal microscopy (Figure 4c, d) and external morphology quantified from high-resolution phase-contrast microscopy images (Figure 4e). As expected, parental and control puro cells gave rise to similar numbers of acini with a central lumen and a typical spherical structure (Figure 4c-e). In contrast, HER2 overexpression resulted in a 4-fold increase in acini lacking a central lumen (Figure 4d) and a 3-fold increase in acini exhibiting branched morphology (Figure 4e) compared to puro control, in line with previous studies.[27, 33] This 3D morphology was similar to that of Bag-1L-overexpressing clones.

Growth of MCF-10A cells requires insulin-like growth factor 1 (IGF-1),[34] which is chemically and functionally similar to insulin and facilitates cellular glucose uptake.[35] Overexpression of HER2 causes metabolic transformation of MCF-10A cells, which is characterised by insulin-independent proliferation and enhances glucose uptake in the absence of IGF-1 receptor activity.[3, 20, 37] Based on the phenotypic similarities between HER2- and Bag-1L-overexpressing MCF10A cells in 3D, we investigated whether the atypical phenotype of Bag-1L-overexpressing MCF-10A clones could also be due to metabolic changes associated with loss of responsiveness to insulin. To this end, cells were cultured in insulin-free or insulin-containing media using HER2-overexpressing MCF-10A clones as a control. In line with previous studies,[3] no significant difference in the growth of HER2-overexpressing clones was observed under these conditions (Figure 4f). Conversely, growth of puro and pcDNA controls, displayed a significant increase of ~1.4-fold in the presence compared to the absence of insulin (Figure 4f). Similarly, a growth increase of ~1.6-fold in Bag-1L/A and ~1.5-

fold in Bag-1L/B was observed in the presence compared to the absence of insulin indicating responsiveness to this hormone. Moreover, all cell lines were responsive to EGF for growth (Figure 4f), consistently with previous reports.[20] These data suggest that the mechanism responsible for the morphological changes observed in response to Bag-1L overexpression is likely to be different to that of HER2 and requires further investigation.

Effect of Bag-1 inhibitors on 2D culture and acini morphogenesis

To confirm the functional consequences of Bag-1L overexpression on 2D growth, MCF-10A clones were examined in the presence of Thioflavin S and Thio-2 inhibitors of Bag-1 protein-protein interactions.[12, 39] Viability assay data show that Thio-2 significantly decreased growth across all cell lines at 50 µM and 100 µM, while Thioflavin S had no effect (Figure 5a), confirming our previously published findings.[12] Therefore, Thio-2 was used in subsequent experiments.

We examined whether the atypical morphology of Bag-1L-overexpressing acini could be pharmacologically reversed. MCF-10A cells grown in 2D were pre-treated with Thio-2 for 24 h before seeding on Matrigel with additional treatments administered on days 4 and 8 of 3D culture. Thio-2 treatment significantly reduced the number of atypical acini by 17% in Bag-1L/A and 29% in Bag-1L/B compared to DMSO control (Figure 5b). Acini displaying atypical external morphology exhibited a reduced level of branching (Figure 5c) suggesting that changes in morphology could be due to Bag-1 protein-protein interactions. Furthermore, upon serum stimulation of serum-deprived cells there was no noticeable inhibitory effect by Thio-2 treatment on the activities of ERK and AKT as shown by immunoblot analysis (Figure 5d). This could explain the lack of luminal clearing observed in Bag-1 overexpressing acini and is consistent with findings by Anderson *et al.*[2] who showed that ERK activity needs to be blocked by U0126 in order for luminal clearing to occur in Bag-1 overexpressing acini.

Discussion

Our data demonstrate, for the first time, that overexpression of the Bag-1L isoform alone is sufficient to suppress luminal apoptosis and drives the formation of MCF-10A acini with a branched morphology, which resemble transformed acini formed by HER2-overexpressing MCF-10A cells generated here by us, and published by others.[27, 33] Although studies by Anderson *et al.* [2] revealed the existence of reduced luminal clearing in acini co-overexpressing all three main Bag-1 isoforms (Bag-1S, Bag-1M, Bag-1L) no observation of abnormal branced morphology was reported. Similar to previous observations in non-tumourigenic HaCaT skin epidermal keratinocytes,[19] our data also show that Bag-1L overexpression results in decreased MCF-10A cell growth in 2D cultures, an event which seems to be inversely correlated to its level of expression.

MCF-10A acini morphogenesis proceeds through a highly regulated sequence of events. Cell detachment from the BM in the lumen of acini induces cellular stresses resulting in anoikis and luminal clearing. This occurs through downregulation of ERK activity, resulting in potentiation of the pro-apoptotic activity of Bim_{EL}.[8-10, 36] Studies by Anderson *et al.*[2] in which Bag-1S, Bag-1M, and Bag-1L isoforms were co-expressed in MCF-10A cells reveal that this process can be impeded by targeting the pro-apoptotic protein Bim_{EL} for proteasomal degradation through enhanced activation of the RAF-1/MEK/ERK signalling cascade. Although Thio-2 is known to downregulate the activity of ERK,[12] and could partially reverse the branched acini morphology driven by Bag-1L overexpression, it did not induce anoikis of luminal cells. Studies by Debnath *et al.*[8] have shown that apoptosis inhibition alone is insufficient to prevent luminal clearing, with Bcl-2 overexpression delaying but not completely preventing anoikis; this has implicated the existence of an additional metabolic mechanism involving the upregulation of cellular anti-oxidant defences.[7, 37] To investigate the possibility that Bag-1L overexpression may suppress the metabolic impairments associated with detachment from the BM we examined insulin-stimulated growth based on the phenotypic resemblance observed between Bag-1L- and HER2-overexpressing acini. Although HER2

upregulation enhances glucose uptake independently of IGF-1 or insulin, leading to insulin insensitivity,[3] Bag-1L-overexpression retained insulin responsiveness, indicating an inability for glucose uptake independently of insulin. This suggests that despite the phenotypic similarities, Bag-1L-overexpressing acini can overcome the metabolic defects associated with detachment via a different transforming mechanism to HER2.

Targeting Bag-1 with its protein-protein interaction inhibitor Thio-2 attenuated the atypical branching of acini, suggesting that Bag-1L protein-protein interactions are important for determining the morphology displayed upon cell attachment to the BM. Importantly, the level of Bag-1L overexpression correlated with the phenotypic effect of compound treatment as Bag-1L/B clone exhibited the greatest reversal in morphology in response to treatment with Thio-2, thereby providing further evidence of a Bag-1L-driven phenotype. Although Anderson *et al.*[2] described an inability of acini co-overexpressing Bag-1S, Bag-1M and Bag-1L to form a lumen, they did not report formation of a branched external morphology. This could be attributed to the regulatory balance exerted by the combined activities of individual Bag-1 isoforms on cell-to-cell contact. Evidence for this comes from studies by Hinnit *et al.*[19] who measured single-cell movement from small colonies of HGF-stimulated HaCaT cells using scatter assays. They show that constitutive Bag-1L overexpression results in greater than 2-fold cell-to-cell dissociation, whereas Bag-1S and Bag-1M retain their cell-to-cell contacts and exhibit no scattering. When considered together with findings by Hinnit *et al.* and Anderson *et al.*, our data emphasise the importance of the combined activities of distinct Bag-1 isoforms on cellular function, and support a role for Bag-1L in the formation of a premalignant phenotype, that might potentially be amenable to therapeutic intervention.

In summary, our data describe a role for the Bag-1L isoform as a driver of phenotypic changes associated with a premalignant state in the breast using a 3D model of DCIS. Such changes seen in 3D models highlight the efficacy of these models to test the effects of inhibitors of breast tumour initiation in 3D that may not be seen in 2D. The ability of Thio-2 to

reverse some of these changes highlights the potential of Bag-1L-overexpressing MCF-10A acini as a model to test the effect of inhibitors of breast tumour initiation.

Materials and Methods

Cell culture and generation of stable clones

MCF-10A cells were obtained from LGC Standards (Middlesex, UK) and were cultured and maintained as described by Debnath *et al.*.[9] To generate Bag-1L clones, pcDNA3-Bag-1L or empty pcDNA3 vector were transfected into MCF-10A cells using FuGene HD (Promega, UK) and stable integrants selected with Geneticin (100 µg/ml; Sigma, UK). Single clones were harvested by trypsinisation using cloning rings and expanded. HER2 clones were generated as described by Debnath *et al.*.[9] Briefly, MCF-10A cells were infected using 0.45 µm filtered viral supernatant derived from Phoenix HEK-293 cells transfected with pBABEpuro-HER2 vector[18] (Addgene plasmid 40978), and were selected with puromycin (0.5 µg/ml). Resistant clones were pooled together by trypsinisation and expanded.

Immunocytochemistry, image acquisition, and scoring of acini

For 2D immunofluorescence staining, cells were plated on type I rat tail collagen-coated (10 µg/ml) glass coverslips and processed as previously described.[19] Acini were grown in 8 well culture slides (BD Falcon, UK) and were fixed in paraformaldehyde (2% v/v final conc.), which was added directly into culture media to minimise acini loss through aspiration; staining was performed as described by Debnath *et al.*.[9] Immunodetection was performed using antibodies raised against Ki67 (Abcam, UK), HER2 (CST, UK), keratin 18 Asp396 neo-epitope (M30 CytoDEATH^{TM} mAb, Enzo Life Sciences, UK), and Bag-1 (TB3 pAb, made in house [4]); phalloidin-TRITC (Dako, UK) was used to stain the cytoskeleton and nuclei were stained with 4'6-diamidino-2-phenylindole (DAPI; Sigma, UK). Secondary antibodies were Alexa Fluor® 488 goat anti-mouse IgG and Alexa Fluor® 546 goat anti-rabbit IgG (Life technologies, UK). Imaging of 2D cultures was performed with an Olympus IX81 microscope. To quantify the external morphology of acini, mounted slides were viewed using an Olympus BX51 microscope with an automated slide scanning system (Olympus Soft Imaging Systems,

Munster, Germany) and high-resolution pictures covering the entire sample were captured using dotSlide v2.2 (Olympus Soft Imaging Solutions, GmbH). Images were viewed with Olympus OlyVIA v2.4 and morphology was scored by manual counting. To score acini luminal clearing or morphology, cross-sectional examination of all acini within each chamber was performed with a Leica SP5 confocal microscope; representative images were captured and analysed with LEICA LAS AF v2.6.0.

Immunoblotting

Lysates of 2D or 3D cultures were prepared in ice cold protease-supplemented (Sigma, UK) RIPA buffer (CST, UK). Acini extracts were dissociated through a 27-gauge needle and cleared by centrifugation (13,000 rpm, 15 min, 4°C). SDS-PAGE and immunoblotting were conducted according to standard protocols.[17] Immunodetection was performed using antibodies raised against Bag-1 (3.10 G3E2, Santa Cruz Biotechnology, UK), HER2, p44/p42 MAPK (ERK1/2) (CST), phospho-p44/p42 MAPK (P-ERK1/2) (Thr202/Tyr204) (20G11) (CST), AKT (CST) and P-AKT Ser473 (CST). Anti-β-actin-HRP was from Sigma and secondary HRP-conjugated immunoglobulins were from Dako. Images were acquired with a BioRad Fluor-S^{TM} MultiImager using Quantity One analysis software v4.6.3. Quantification of bands was performed using the volume tools in Quantity One analysis software v4.6.6 (where a volume is the sum of the intensities of the pixels within the volume boundary, times by the pixel area). Analysis was carried out on bands pre-saturation. All bands were adjusted for global background volume. Protein abundance was calculated by normalising bands for actin, and expressed relative to pcDNA.

Cell growth assays

To measure growth, 20,000 cells/well were seeded in triplicate in 12 well plates and were fixed in ice cold methanol. Fixed cells were stained with 0.1% crystal violet and the

associated dye dissolved in 20% acetic acid to measure absorbance at 595 nm. For insulin and EGF responsiveness assays, cells which had been serum and growth factor starved for 24 h were grown in the absence or presence of the relative growth factor for 48 h and were subsequently fixed in ice cold methanol and stained with 0.1% (w/v) crystal violet. The associated dye was extracted in 20% acetic acid and the absorbance at 595 nm was expressed relative to that of the growth factor-free condition.

Bag-1 inhibition

For dose-response experiments, 3,000 cells/well were seeded in triplicate in 96-well plates and were treated with DMSO, Thioflavin S (Sigma, UK) or Thio-2 (ref. 12) for 5 days. Cell viability was determined by CellTitre 96 Aqueous One solution assay (Promega) according to the manufacturer's protocol. For acini morphogenesis assays, cells were pre-treated with compounds in 2D 24 h before seeding in compound-free assay media in 3D. Acini were fed with compound-containing assay media on days 4 and 8 of culture. To examine the effect of Thio-2 on signalling cell monolayers were rinsed with PBS and kept for 4 h in insulin and EGF free media containing reduced horse serum (0.5%). Cells were subsequently treated with compounds for 1 h and lysates were prepared after 10 min of horse serum (10%) stimulation. Unstimulated cells were used as negative controls for protein activation, while the MEK inhibitor U0126 (Promega) was used as a positive control for inhibition of ERK activity.

Statistical analysis

Statistical analysis was performed using GraphPad Prism version 6.00 (GraphPad Software, San Diego, USA) for Windows. Analyses of more than two groups were done using 2-way ANOVA with Bonferroni's multiple comparisons test.

Acknowledgements

The authors thank Dr David Johnston (Biomedical Imaging Unit, Faculty of Medicine, University of Southampton and University Hospital Southampton NHS Foundation Trust) for help with confocal microscopy and slide scanning. RIC and ESP (project grant reference: 2011NovPR39), and JPB (project grant reference: 2010NovPR12) are funded by Breast Cancer Campaign (BCC). CRB is funded by the Medical Research Council (MR/J004103/1) and Cancer Research UK (C34999/A15992). The authors thank Professor G. Packham for critical review of the manuscript.

References

1 Afentakis M, Dowsett M, Sestak I, Salter J, Howell T, Buzdar A *et al* (2013). Immunohistochemical BAG1 expression improves the estimation of residual risk by IHC4 in postmenopausal patients treated with anastrazole or tamoxifen: a TransATAC study. *Breast Cancer Res Treat* **140:** 253-262.

2 Anderson LR, Sutherland RL, Butt AJ (2010). BAG-1 overexpression attenuates luminal apoptosis in MCF-10A mammary epithelial cells through enhanced RAF-1 activation. *Oncogene* **29:** 527-538.

3 Bollig-Fischer A, Dewey TG, Ethier SP (2011). Oncogene Activation Induces Metabolic Transformation Resulting in Insulin-Independence in Human Breast Cancer Cells. *PLoS ONE* **6:** e17959.

4 Brimmell M, Burns JS, Munson P, McDonald L, O'Hare MJ, Lakhani SR *et al* (1999). High level expression of differentially localized BAG-1 isoforms in some oestrogen receptor-positive human breast cancers. *Br J Cancer* **81:** 1042-1051.

5 Burstein HJ, Polyak K, Wong JS, Lester SC, Kaelin CM (2004). Ductal carcinoma in situ of the breast. *New England Journal of Medicine* **350:** 1430-1441.

6 Cutress RI, Townsend PA, Sharp A, Maison A, Wood L, Lee R *et al* (2003). The nuclear BAG-1 isoform, BAG-1L, enhances oestrogen-dependent transcription. *Oncogene* **22:** 4973-4982.

7 Davison CA, Durbin SM, Thau MR, Zellmer VR, Chapman SE, Diener J *et al* (2013). Antioxidant enzymes mediate survival of breast cancer cells deprived of extracellular matrix. *Cancer Res* **73:** 3704-3715.

8 Debnath J, Mills KR, Collins NL, Reginato MJ, Muthuswamy SK, Brugge JS (2002). The role of apoptosis in creating and maintaining luminal space within normal and oncogene-expressing mammary acini. *Cell* **111:** 29-40.

9 Debnath J, Muthuswamy SK, Brugge JS (2003). Morphogenesis and oncogenesis of MCF-10A mammary epithelial acini grown in three-dimensional basement membrane cultures. *Methods* **30:** 256-268.

10 Debnath J, Brugge JS (2005). Modelling glandular epithelial cancers in three-dimensional cultures. *Nat Rev Cancer* **5:** 675-688.

11 Enthammer M, Papadakis ES, Gachet MS, Deutsch M, Schwaiger S, Koziel K *et al* (2013). Isolation of a Novel Thioflavin S-Derived Compound that Inhibits BAG-1-Mediated Protein Interactions and Targets BRAF Inhibitor-Resistant Cell Lines. *Molecular cancer therapeutics*.

12 Enthammer M, Papadakis ES, Salome Gachet M, Deutsch M, Schwaiger S, Koziel K *et al* (2013). Isolation of a novel thioflavin S-derived compound that inhibits BAG-1-mediated protein interactions and targets BRAF inhibitor-resistant cell lines. *Molecular cancer therapeutics* **12:** 2400-2414.

13 Fournier MV, Martin KJ, Kenny PA, Xhaja K, Bosch I, Yaswen P *et al* (2006). Gene Expression Signature in Organized and Growth-Arrested Mammary Acini Predicts Good Outcome in Breast Cancer. *Cancer research* **66:** 7095-7102.

14 Froesch BA, Takayama S, Reed JC (1998). BAG-1L protein enhances androgen receptor function. *J Biol Chem* **273:** 11660-11666.

15 Gerdes J, Lemke H, Baisch H, Wacker HH, Schwab U, Stein H (1984). Cell cycle analysis of a cell proliferation-associated human nuclear antigen defined by the monoclonal antibody Ki-67. *The Journal of Immunology* **133:** 1710-1715.

16 Grassian AR, Schafer ZT, Brugge JS (2011). ErbB2 stabilizes epidermal growth factor receptor (EGFR) expression via Erk and Sprouty2 in extracellular matrix-detached cells. *J Biol Chem* **286:** 79-90.

17 Green MR, Sambrook J (2012). *Molecular cloning : a laboratory manual*. Cold Spring Harbor Laboratory Press: Cold Spring Harbor, N.Y.

18 Greulich H, Kaplan B, Mertins P, Chen TH, Tanaka KE, Yun CH *et al* (2012). Functional analysis of receptor tyrosine kinase mutations in lung cancer identifies oncogenic extracellular domain mutations of ERBB2. *Proc Natl Acad Sci U S A* **109:** 14476-14481.

19 Hinitt CA, Wood J, Lee SS, Williams AC, Howarth JL, Glover CP *et al* (2010). BAG-1 enhances cell-cell adhesion, reduces proliferation and induces chaperone-independent suppression of hepatocyte growth factor-induced epidermal keratinocyte migration. *Experimental cell research* **316:** 2042-2060.

20 Ignatoski KM, Lapointe AJ, Radany EH, Ethier SP (1999). erbB-2 overexpression in human mammary epithelial cells confers growth factor independence. *Endocrinology* **140:** 3615-3622.

21 Kenny PA, Lee GY, Myers CA, Neve RM, Semeiks JR, Spellman PT *et al* (2007). The morphologies of breast cancer cell lines in three-dimensional assays correlate with their profiles of gene expression. *Molecular oncology* **1:** 84-96.

22 Knee DA, Froesch BA, Nuber U, Takayama S, Reed JC (2001). Structure-function analysis of Bag1 proteins. Effects on androgen receptor transcriptional activity. *J Biol Chem* **276:** 12718-12724.

23 Kudoh M, Knee DA, Takayama S, Reed JC (2002). Bag1 proteins regulate growth and survival of ZR-75-1 human breast cancer cells. *Cancer Res* **62:** 1904-1909.

24 Lee SS, Crabb SJ, Janghra N, Carlberg C, Williams AC, Cutress RI *et al* (2007). Subcellular localisation of BAG-1 and its regulation of vitamin D receptor-mediated transactivation and involucrin expression in oral keratinocytes: Implications for oral carcinogenesis. *Experimental cell research* **313:** 3222-3238.

25 Martin KJ, Patrick DR, Bissell MJ, Fournier MV (2008). Prognostic Breast Cancer Signature Identified from 3D Culture Model Accurately Predicts Clinical Outcome across Independent Datasets. *PLoS ONE* **3:** e2994.

26 Millar EK, Anderson LR, McNeil CM, O'Toole SA, Pinese M, Crea P *et al* (2009). BAG-1 predicts patient outcome and tamoxifen responsiveness in ER-positive invasive ductal carcinoma of the breast. *Br J Cancer* **100:** 123-133.

27 Muthuswamy SK, Li D, Lelievre S, Bissell MJ, Brugge JS (2001). ErbB2, but not ErbB1, reinitiates proliferation and induces luminal repopulation in epithelial acini. *Nature cell biology* **3:** 785-792.

28 Nadler Y, Camp RL, Giltnane JM, Moeder C, Rimm DL, Kluger HM *et al* (2008). Expression patterns and prognostic value of Bag-1 and Bcl-2 in breast cancer. *Breast Cancer Res* **10:** R35.

29 Packham G, Brimmell M, Cleveland JL (1997). Mammalian cells express two differently localized Bag-1 isoforms generated by alternative translation initiation. *Biochem J* **328 (Pt 3):** 807-813.

30 Paik S, Shak S, Tang G, Kim C, Baker J, Cronin M *et al* (2004). A multigene assay to predict recurrence of tamoxifen-treated, node-negative breast cancer. *N Engl J Med* **351:** 2817-2826.

31 Parker JS, Mullins M, Cheang MC, Leung S, Voduc D, Vickery T *et al* (2009). Supervised risk predictor of breast cancer based on intrinsic subtypes. *J Clin Oncol* **27:** 1160-1167.

32 Petersen OW, Rønnov-Jessen L, Howlett AR, Bissell MJ (1992). Interaction with basement membrane serves to rapidly distinguish growth and differentiation pattern of normal and malignant human breast epithelial cells. *Proceedings of the National Academy of Sciences* **89:** 9064-9068.

33 Pradeep CR, Zeisel A, Kostler WJ, Lauriola M, Jacob-Hirsch J, Haibe-Kains B *et al* (2012). Modeling invasive breast cancer: growth factors propel progression of HER2-positive premalignant lesions. *Oncogene* **31:** 3569-3583.

34 Ram TG, Kokeny KE, Dilts CA, Ethier SP (1995). Mitogenic activity of neu differentiation factor/heregulin mimics that of epidermal growth factor and insulin-like growth factor-I in human mammary epithelial cells. *Journal of cellular physiology* **163:** 589-596.

35 Rechler MM, Nissley SP (1985). The nature and regulation of the receptors for insulin-like growth factors. *Annual review of physiology* **47:** 425-442.

36 Reginato MJ, Mills KR, Becker EBE, Lynch DK, Bonni A, Muthuswamy SK *et al* (2005). Bim Regulation of Lumen Formation in Cultured Mammary Epithelial Acini Is Targeted by Oncogenes. *Molecular and Cellular Biology* **25:** 4591-4601.

37 Schafer ZT, Grassian AR, Song L, Jiang Z, Gerhart-Hines Z, Irie HY *et al* (2009). Antioxidant and oncogene rescue of metabolic defects caused by loss of matrix attachment. *Nature* **461:** 109-113.

38 Schneikert J, Hubner S, Martin E, Cato AC (1999). A nuclear action of the eukaryotic cochaperone RAP46 in downregulation of glucocorticoid receptor activity. *J Cell Biol* **146:** 929-940.

39 Sharp A, Crabb SJ, Johnson PW, Hague A, Cutress R, Townsend PA *et al* (2009). Thioflavin S (NSC71948) interferes with Bcl-2-associated athanogene (BAG-1)-mediated protein-protein interactions. *J Pharmacol Exp Ther* **331:** 680-689.

40 Sharp A, Cutress RI, Johnson PW, Packham G, Townsend PA (2009). Short peptides derived from the BAG-1 C-terminus inhibit the interaction between BAG-1 and HSC70 and decrease breast cancer cell growth. *FEBS Lett* **583:** 3405-3411.

41 Shatkina L, Mink S, Rogatsch H, Klocker H, Langer G, Nestl A *et al* (2003). The cochaperone Bag-1L enhances androgen receptor action via interaction with the NH2-terminal region of the receptor. *Mol Cell Biol* **23:** 7189-7197.

42 Slamon DJ, Clark GM, Wong SG, Levin WJ, Ullrich A, McGuire WL (1987). Human breast cancer: correlation of relapse and survival with amplification of the HER-2/neu oncogene. *Science* **235:** 177-182.

43 Takayama S, Krajewski S, Krajewska M, Kitada S, Zapata JM, Kochel K *et al* (1998). Expression and location of Hsp70/Hsc-binding anti-apoptotic protein BAG-1 and its variants in normal tissues and tumor cell lines. *Cancer Res* **58:** 3116-3131.

44 Tang SC, Shehata N, Chernenko G, Khalifa M, Wang X, Shaheta N (1999). Expression of BAG-1 in invasive breast carcinomas. *J Clin Oncol* **17:** 1710-1719.

45 Tang SC, Beck J, Murphy S, Chernenko G, Robb D, Watson P *et al* (2004). BAG-1 expression correlates with Bcl-2, p53, differentiation, estrogen and progesterone receptors in invasive breast carcinoma. *Breast Cancer Res Treat* **84:** 203-213.

46 Townsend PA, Cutress RI, Sharp A, Brimmell M, Packham G (2003). BAG-1: a multifunctional regulator of cell growth and survival. *Biochimica et biophysica acta* **1603:** 83-98.

47 Turner BC, Krajewski S, Krajewska M, Takayama S, Gumbs AA, Carter D *et al* (2001). BAG-1: a novel biomarker predicting long-term survival in early-stage breast cancer. *J Clin Oncol* **19:** 992-1000.

48 Yang X, Hao Y, Ding Z, Pater A, Tang SC (1999). Differential expression of antiapoptotic gene BAG-1 in human breast normal and cancer cell lines and tissues. *Clinical cancer research : an official journal of the American Association for Cancer Research* **5:** 1816-1822.

Figure legends

Figure 1. Effect of Bag-1L overexpression on MCF-10A 2D cultures

Bag-1 protein expression was examined in MCF-10A clones grown in 2D cultures as indicated by: (**a**) Immunoblot where β-actin was included as a control for loading and (**b**) immunocytochemical labelling for Bag-1 (red) and nuclear counterstain DAPI (blue); two exposure times are shown for Bag-1 staining; scale bars = 50 μm. (**c**) Phase-contrast images reveal that Bag-1L-overexpressing clones acquire a cobblestone morphology which is typical of MCF-10A cells. Scale bars = 200 μm. (**d**) The colony-forming efficiency of Bag-1L clones was assessed in a clonogenic assay and expressed as the plating efficiency. Values represent the mean ± SEM from three independent experiments with triplicate determinations. (**e**) Proliferation of clones was measured at days 2 and 4 of culture. Cells (20,000 per well) were plated at day 0 and were fixed and stained with crystal violet. Stain was dissolved in 20% acetic acid and absorbance at 595 nm recorded. Bar graphs represent the mean ± SEM values from three independent experiments with triplicate determinations. * $p \leq 0.05$, ** $p \leq 0.01$ as determined by 2-way ANOVA with Bonferroni's multiple comparisons.

Figure 2. Bag-1L overexpression attenuates luminal clearing and promotes an abnormal acinar morphology

(**a**) Immunoblot analysis showing expression of Bag-1 isoforms in lysates from MCF-10A acini clones cultured for 12 days; β-actin was included as a loading control. Densitometric analysis shows the abundance of Bag-1S and Bag-1L protein isoforms relative to pcDNA control. (**b**) Representative confocal immunofluorescence images taken through the centre of MCF-10A acini at day 20 of culture. Cells were stained with phalloidin-TRITC (green) and nuclei counterstained with DAPI (red); scale bars = 100 μm. (**c**) Acini with filled lumens were counted at day 20 of growth and their number is expressed as a percentage of total acini. (**d**) Representative phase-contrast images of MCF-10A cell clones grown in 3D for 20 days

revealing gross external morphology. White scale bars = 500 μm; black scale bars = 200 μm. (**e**) Acini with abnormal morphology were counted at day 20 of growth and their number is expressed as a percentage of total acini. Values represent the mean ± SEM from at least three independent experiments with duplicate determinations. * $p \leq 0.05$, ** $p \leq 0.01$, **** $p \leq 0.0001$ as determined by 2-way ANOVA with Bonferroni's multiple comparisons.

Figure 3. Bag-1L overexpression does not prevent cell cycle arrest but attenuates luminal apoptosis during acini morphogenesis

Representative confocal immunofluorescence images taken through the centre of MCF-10A acini at the indicated time points of 3D morphogenesis. (**a**) Proliferation was examined using Ki67 (green) as a marker. (**b**) Apoptosis was assessed using M30 (green) as a marker of caspase-cleaved cytokeratin 18. Nuclei were counterstained with DAPI (red); scale bars = 50 μm.

Figure 4. HER2 overexpression promotes atypical MCF-10A morphology in 3D and insulin unresponsiveness in 2D cultures

(**a**) Immunoblot analysis of HER2 overexpression in retrovirally-transduced MCF-10A pooled clones grown in 2D culture. Actin was included as a control for loading. (**b**) Immunofluorescence staining for HER2 (red) in 2D cultures of MCF-10A parental or retrovirally transduced with pBabe-puro vector control or pBabe-puro/HER2; nuclei were counterstained with DAPI (blue), while secondary antibody alone was used to exclude non-specific staining; scale bars = 50 μm. (**c**) Representative confocal immunofluorescence images of MCF-10A acini at day 12 of growth on Matrigel. Acini were stained with phalloidin-TRITC (green) and nuclei counterstained with DAPI (red); scale bars = 50 μm. The number of acini with (**d**) filled lumens (day 12) or (**e**) abnormal morphology (day 20) was counted and is expressed as a percentage of the total number of acini. Values represent the mean ± SEM

from three independent experiments with quadruplicate determinations. ** $p \leq 0.01$, **** $p \leq 0.0001$ as determined by 2-way ANOVA with Bonferroni's multiple comparisons. (**f**) Insulin and EGF sensitivity was assessed in 2D culture under serum-free conditions (24 h serum starvation) following treatment for 48 h as indicated. Bar graphs represent the mean fold change ± SEM in cell growth in growth factor-supplemented relative to growth factor-free media for each cell line, which was determined by crystal violet assay. Data are from at least three independent experiments with triplicate determinations. * $p \leq 0.05$, ** $p \leq 0.01$, *** $p \leq 0.001$, **** $p \leq 0.0001$ as determined by 2-way ANOVA with Bonferroni's multiple comparisons.

Figure 5. Thio-2 can partially reverse the abnormal acinar morphology associated with Bag-1L overexpression

(**a**) MCF-10A cells were treated with Thioflavin S or Thio-2 at the indicated concentrations for 5 days and viability was assessed by CellTiter Aqueous One solution assay relative to DMSO-treated cells at each concentration. Values represent the mean ± SD as percent of control from three experiments with triplicate determinations. **** $p \leq 0.0001$ was determined by 2-way ANOVA with Bonferroni's multiple comparisons relative to the effect of the lowest concentration of Thio-02 on each corresponding cell. (**b**) MCF-10A cells were treated for 24 h with Thio-2 (50 μM) or DMSO (0.5% v/v) before seeding on Matrigel and acini were allowed to form over 14 days; further treatment (25 μM Thio-2 or 0.25% v/v DMSO) was administered on days 4 and 8 of 3D culture. Acini exhibiting abnormal morphology were quantified and expressed as a percentage of the total number. Values represent the mean ± SEM from four independent experiments with duplicate determinations. * $p \leq 0.05$, ** $p \leq 0.01$, *** $p \leq 0.001$ as determined by 2-way ANOVA with Bonferroni's multiple comparisons. (c) Representative phase-contrast microscopy images show the atypical branching external morphology of Bag-1L/B is acini in the presence of DMSO or Thio-2. Scale bars = 50 μm. (d) Immunoblot analysis shows the effect of serum (10%) stimulation alone or in in the presence

of DMSO (0.5%), Thio-2 (50 μM), or U0126 (25 μM) on the activation of ERK and AKT in cells that had been serum-deprived. β-actin was used as a loading control.

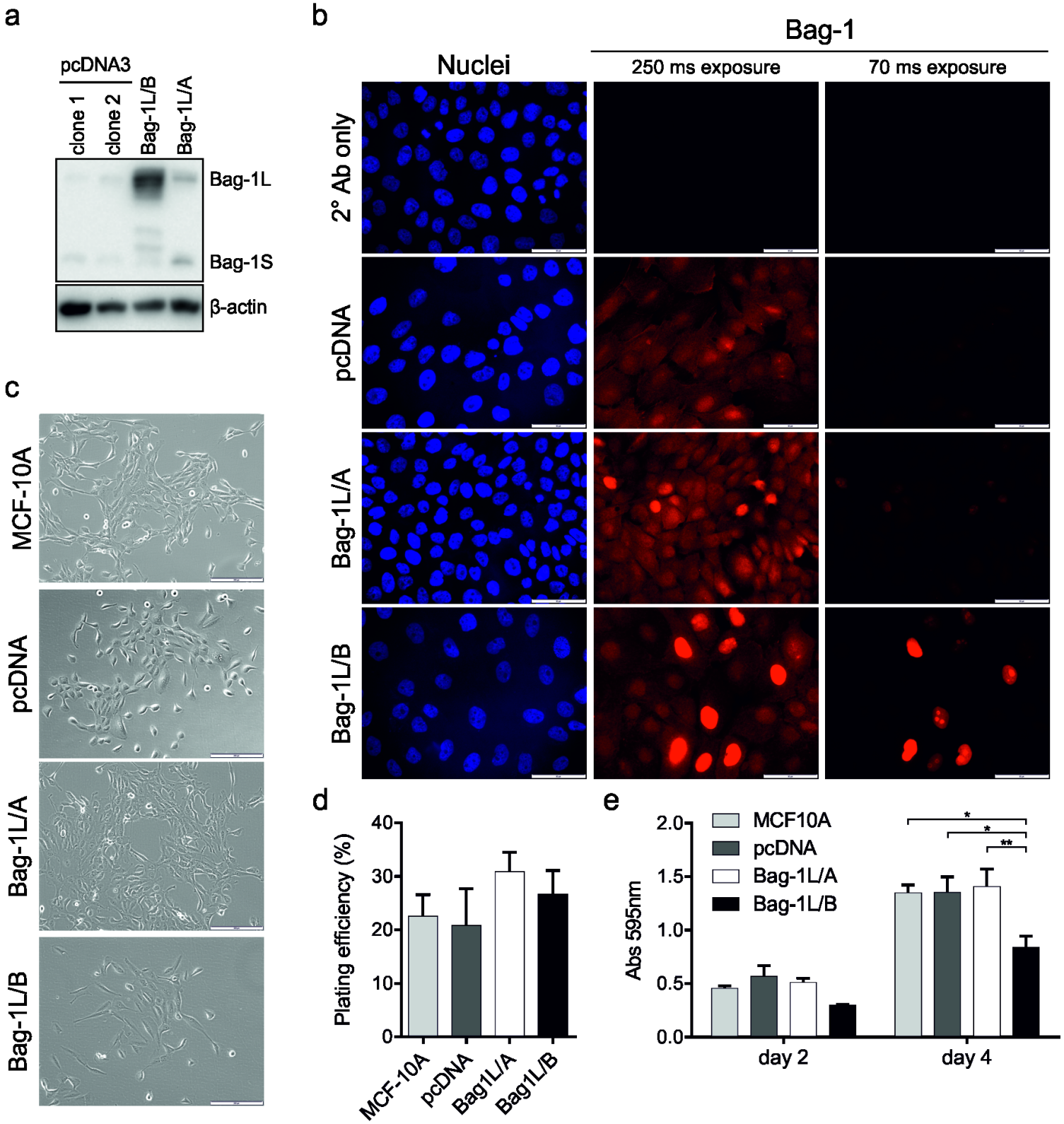
a
pcDNA3
clone 1
clone 2
Bag-1L/B
Bag-1L/A
Bag-1L
Bag-1S
β-actin
b
Bag-1
Nuclei
250 ms exposure
70 ms exposure
2° Ab only
pcDNA
Bag-1L/A
Bag-1L/B
c
MCF-10A
pcDNA
Bag-1L/A
Bag-1L/B
d
Plating efficiency (%)
40
30
20
10
0
MCF-10A
pcDNA
Bag1L/A
Bag1L/B
e
Abs 595nm
2.0
1.5
1.0
0.5
0.0
MCF10A
pcDNA
Bag-1L/A
Bag-1L/B
*
*
**
day 2
day 4

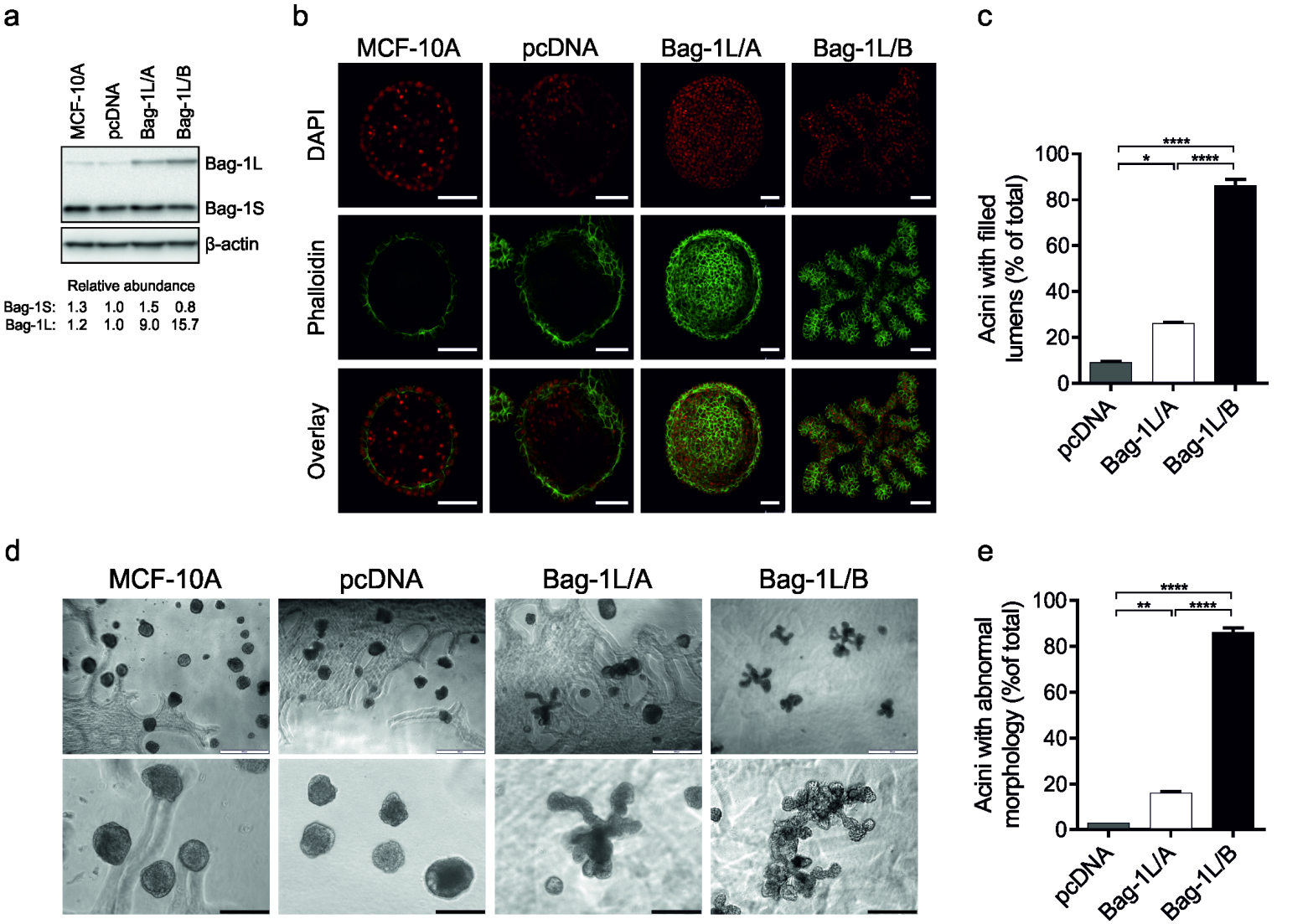
a
MCF-10A
pcDNA
Bag-1L/A
Bag-1L/B
Bag-1L
Bag-1S
β-actin
Relative abundance
Bag-1S: 1.3 1.0 1.5 0.8
Bag-1L: 1.2 1.0 9.0 15.7
b
MCF-10A
pcDNA
Bag-1L/A
Bag-1L/B
DAPI
Phalloidin
Overlay
c
Acini with filled lumens (% of total)
100
80
60
40
20
0
****
*
****
pcDNA
Bag-1L/A
Bag-1L/B
d
MCF-10A
pcDNA
Bag-1L/A
Bag-1L/B
e
Acini with abnormal morphology (%of total)
100
80
60
40
20
0
****
**
****
pcDNA
Bag-1L/A
Bag-1L/B

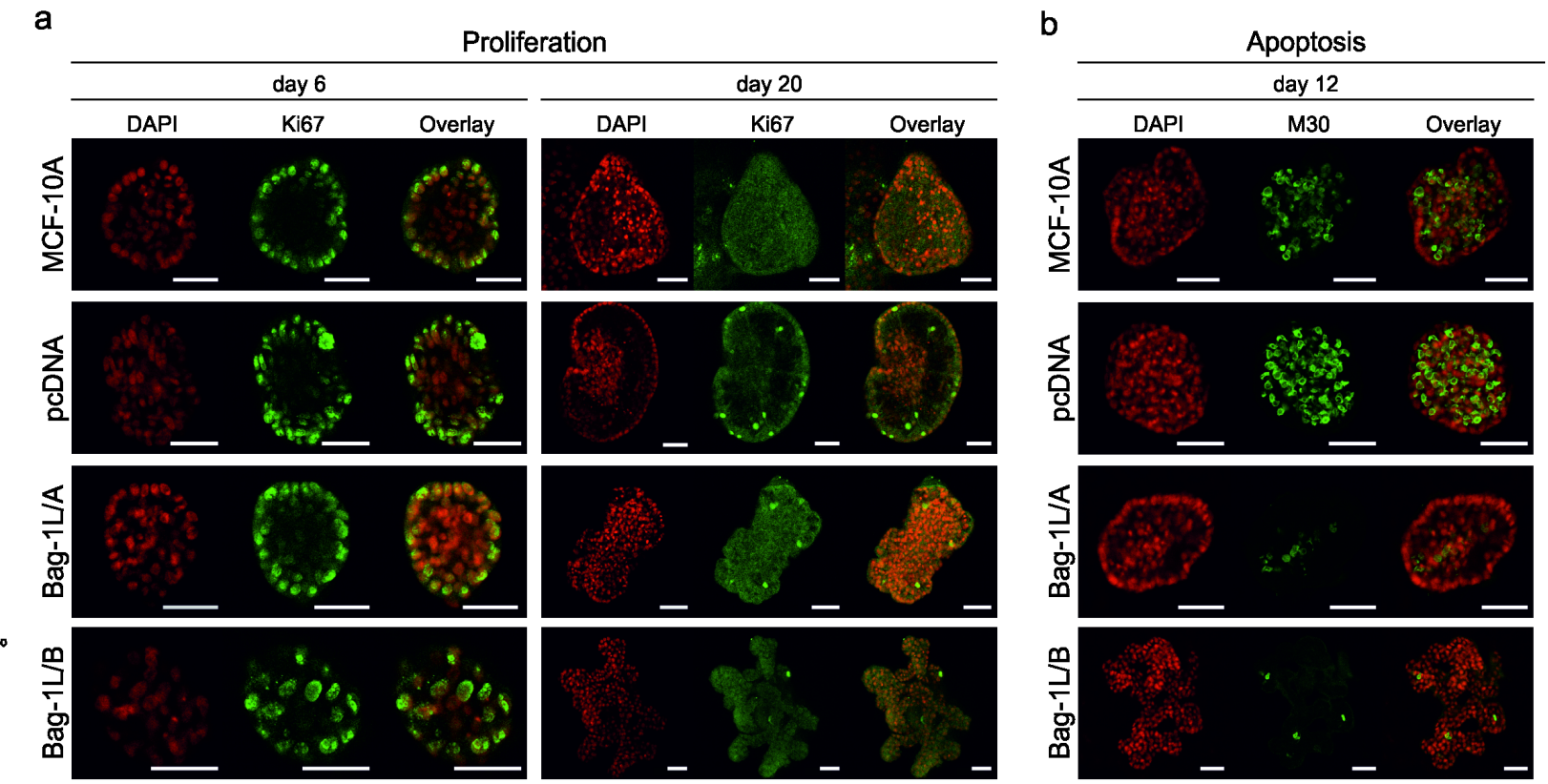
a
Proliferation
day 6
day 20
DAPI
Ki67
Overlay
DAPI
Ki67
Overlay
MCF-10A
pcDNA
Bag-1L/A
Bag-1L/B
b
Apoptosis
day 12
DAPI
M30
Overlay
MCF-10A
pcDNA
Bag-1L/A
Bag-1L/B

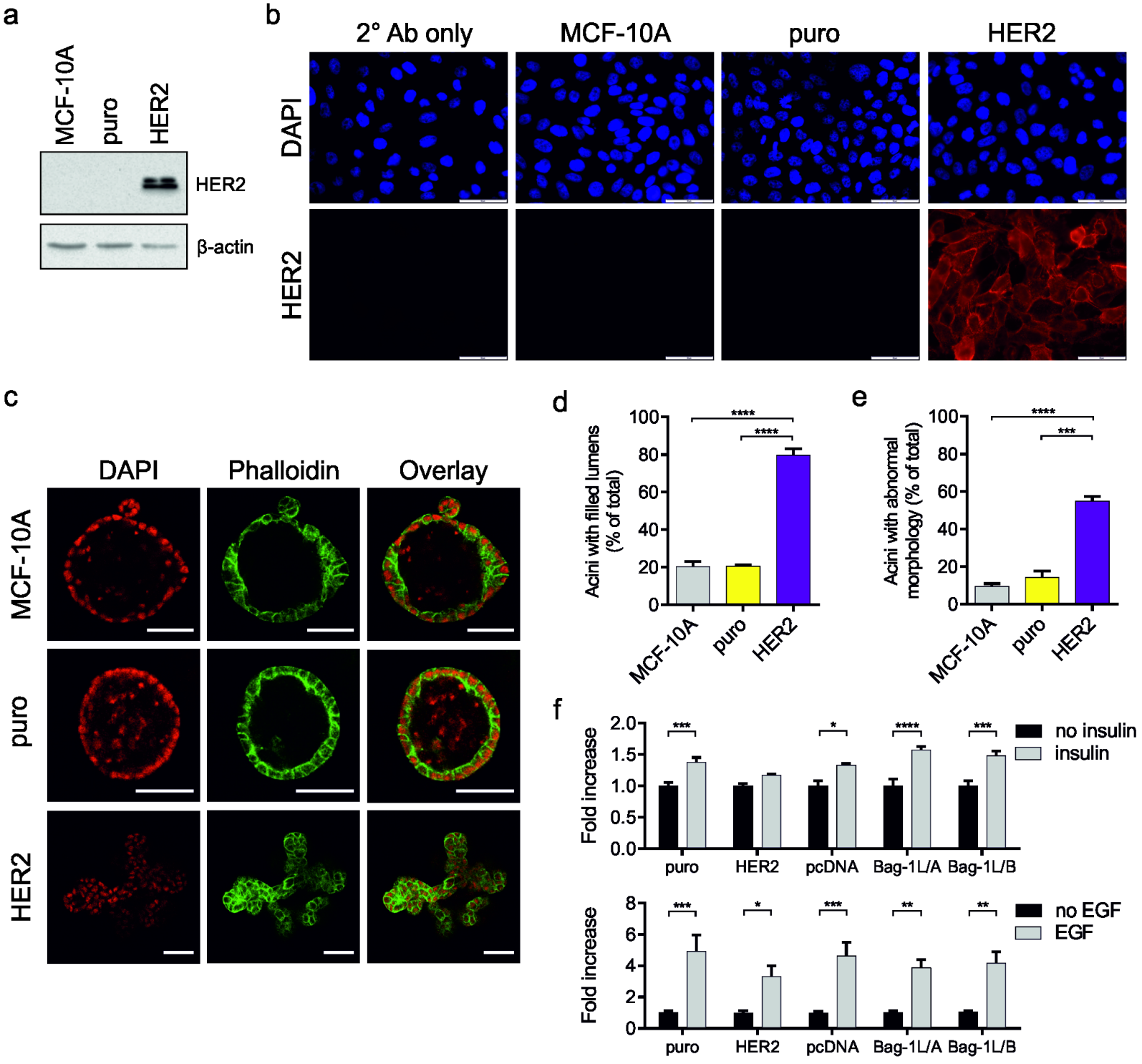
a
MCF-10A
puro
HER2
HER2
β-actin
b
2° Ab only
MCF-10A
puro
HER2
DAPI
HER2
c
DAPI
Phalloidin
Overlay
MCF-10A
puro
HER2
d
Acini with filled lumens (% of total)
100
80
60
40
20
0
****
****
MCF-10A
puro
HER2
e
Acini with abnormal morphology (% of total)
100
80
60
40
20
0
****
***
MCF-10A
puro
HER2
f
Fold increase
2.0
1.5
1.0
0.5
0.0
***
*
****
***
no insulin
insulin
puro
HER2
pcDNA
Bag-1L/A
Bag-1L/B
Fold increase
8
6
4
2
0
***
*
***
**
**
no EGF
EGF
puro
HER2
pcDNA
Bag-1L/A
Bag-1L/B

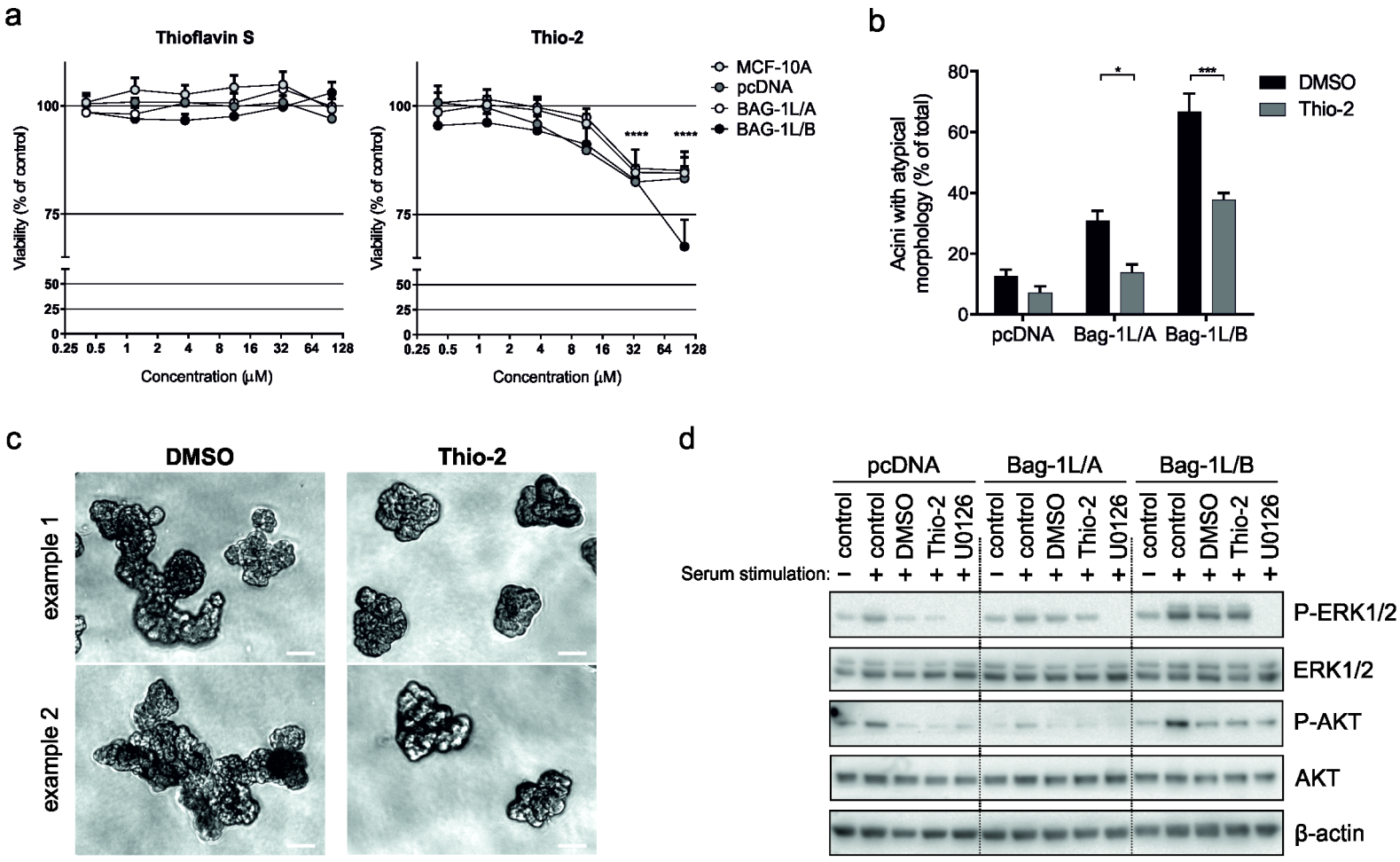
a
Thioflavin S
Thio-2
MCF-10A
pcDNA
BAG-1L/A
BAG-1L/B
Viability (% of control)
Concentration (μM)
0.25 0.5 1 2 4 8 16 32 64 128
****
b
Acini with atypical morphology (% of total)
DMSO
Thio-2
pcDNA
Bag-1L/A
Bag-1L/B
*
***
c
DMSO
Thio-2
example 1
example 2
d
pcDNA
Bag-1L/A
Bag-1L/B
Serum stimulation:
control
DMSO
Thio-2
U0126
P-ERK1/2
ERK1/2
P-AKT
AKT
β-actin